Water Resources Research

RESEARCH ARTICLE
10.1029/2020WR027468

Improving Forecast Skill of Lowland Hydrological Models Using Ensemble Kalman Filter and Unscented Kalman Filter

Y. Sun[1], W. Bao[1], K. Valk[2], C. C. Brauer[2], J. Sumihar[3], and A. H. Weerts[2,3]

[1]Department of Hydrology and Water Resources, Hohai University, Nanjing, China, [2]Hydrology and Quantitative Water Management Group, Wageningen University, Wageningen, the Netherlands, [3]Deltares, Delft, the Netherlands

Key Points:
- The ensemble Kalman filter and unscented Kalman filter are utilized to improve forecast skill of a hydrological model by state estimation
- Both approaches have improved the forecast performance, with unscented Kalman filter being the computationally leaner option
- The unscented Kalman filter can be considered as a new and effective option to assimilate observations into low-dimensional models

Supporting Information:
- Supporting Information S1

Correspondence to:
A. H. Weerts,
albrecht.weerts@deltares.nl

Citation:
Sun, Y., Bao, W., Valk, K., Brauer, C. C., Sumihar, J., & Weerts, A. H. (2020). Improving forecast skill of lowland hydrological models using ensemble Kalman filter and unscented Kalman filter. *Water Resources Research*, *56*, e2020WR027468. https://doi.org/10.1029/2020WR027468

Received 9 MAR 2020
Accepted 29 JUN 2020
Accepted article online 13 JUL 2020

Abstract For operational water management in lowlands and polders (for instance, in the Netherlands), lowland hydrological models are used for flow prediction, often as an input for a real-time control system to steer water with pumps and weirs to keep water levels within acceptable bounds. Therefore, proper initialization of these models is essential. The ensemble Kalman filter (EnKF) has been widely used due to its relative simplicity and robustness, while the unscented Kalman filter (UKF) has received little attention in the operational context. Here, we test both UKF and EnKF using a lowland lumped hydrological model. The results of a reforecast experiment in an operational context using an hourly time step show that when using nine ensemble members, both filters can improve the accuracy of the forecast by updating the state of a lumped hydrological model (Wageningen Lowland Runoff Simulator, WALRUS) based on the observed discharge, while UKF has achieved better performance than EnKF. Additionally, we show that an increase in the ensemble members does not necessarily mean a significant increase in performance. WALRUS model with either UKF or EnKF could be considered for hydrological forecasting for supporting water management of polders and lowlands, with UKF being the computationally leaner option.

1. Introduction

Lowland areas cover a large part of the world with high social and economic values (Brauer et al., 2013) and are more likely to be threatened by the floods (Zhang et al., 2008). Hence, it is crucial to conduct flood forecasting in these areas. Hydrological models have been used for flood forecasting. Some hydrological models such as the HBV-96 model (Lindström et al., 1997), the Tank model (Sugawara, 1974), the SWAT model (Arnold et al., 1998), and the Xinanjiang model (Shi et al., 2013; Zhao, 1992) have been widely used in the context of hydrological modeling. However, most of these models are designed for sloping catchments rather than lowland catchments. Hence, problems can arise when applying these models to lowland areas because lowland catchments have some unique properties in the mechanisms of hydrological processes such the interaction between the groundwater and the surface water (Sophocleous, 2002) and the connection between the saturated zone and the unsaturated zone (Brauer et al., 2016). As a result, lowland rainfall-runoff models have been developed to handle these issues (Deltares, 2013; Guse et al., 2013; Stricker & Warmerdam, 1982; Thompson et al., 2004). For operational water management in lowlands and polders (for instance, in the Netherlands), models such as the Wageningen Lowland Runoff Simulator (WALRUS) (Brauer, Torfs, et al., 2014) and SOBEK-RR (Bruni et al., 2015) are used for flow prediction, often as inputs to real-time control systems to steer water with pumps and weirs to keep water levels within acceptable bounds. WALRUS is a lumped hydrological model for simulating lowland runoff. This model accounts for essential processes in lowland catchments such as groundwater-unsaturated zone coupling and groundwater-surface water feedbacks (Brauer, Torfs, et al., 2014).

While hydrological models are reported to be robust and reliable in the applications of hydrological modeling, it has been generally recognized that the satisfactory application of such a model can be hampered by many factors including uncertainty in the model inputs (Ajami et al., 2007; McMillan et al., 2011; Renard et al., 2010; Vrugt et al., 2008), uncertainty in the model structure (Beven & Binley, 1992; Butts et al., 2004; Refsgaard et al., 2006; Uhlenbrook et al., 1999), and uncertainty in the model parameters (Ajami et al., 2007; Beven, 1993; Kuczera & Parent, 1998; Li et al., 2010; Shen et al., 2012; Vrugt et al., 2003; Wilby, 2005; Yang

et al., 2007). As a result, data assimilation techniques have been developed and used to handle these issues (Liu & Gupta, 2007). In general, these data assimilation techniques can be divided into three types: error correction, parameter estimation (optimization), and state updating (Liu et al., 2012b). In this study, we only focus on the third type. For the first type and the second type, we refer to Ajami et al. (2007), Broersen and Weerts (2005), Gupta et al. (2006), Li et al. (2010), Shen et al. (2012), Smith et al. (2012), and Weerts et al. (2011).

For state estimation, a general framework is to consider the hydrological model from the perspective of a state-space model. One of the best-known techniques for solving the state-space equation is the Kalman filter (KF) (Kalman, 1960). KF is proposed to provide a recursive solution to the discrete-data linear filter problem. However, the standard KF is restricted to linear systems. Due to the nonlinearity of hydrological models, particle filtering (PF) and some nonlinear extensions of KF, such as extended KF (EKF) (Jazwinski, 1970) and ensemble KF (EnKF) (Evensen, 1994), have been used in the context of hydrological modeling. Applications of EKF in the hydrological literature have been reported by Georgakakos (1986), Francois et al. (2003), and Lü et al. (2011). EKF can be considered as a first-order approximation to the optimal form since EKF linearizes the nonlinear system using the first-order approximations (Welch & Bishop, 1995), while such approximations may lead to deterioration in the performance and even divergence after a few iterations (Evensen, 1994; Reichle, McLaughlin, & Entekhabi, 2002; Reichle, Walker, et al., 2002). Despite its central flaw, other problems, such as difficulties when calculating the Jacobian matrix, also limit its applications (Da Ros & Borga, 1997). PF is a Monte Carlo-based sequential data assimilation technique that is not limited to the Gaussian assumption (Arulampalam et al., 2002). Some applications have been seen in the context of state estimation and parameter estimation of hydrological models (Moradkhani, Hsu, et al., 2005; Weerts & el Serafy, 2006). In PF, the sampling importance resampling (SIR) is often used to handle this problem to avoid the degeneracy problem. However, this resampling procedure can lead to the sample impoverishment problem because the SIR algorithm only maintains and duplicates the particles with high weights.

EnKF addresses the approximation problems by incorporating an ensemble of the state generated by the Monte Carlo method (Burgers et al., 1998; Evensen, 1994; van Leeuwen, 1999). Unlike the approximation implemented by local linearization of EKF, EnKF utilizes a Monte Carlo-based sampling strategy to approximate and propagate the probability distribution functions. EnKF has received much attention in the field of hydrology due to its relative simplicity and robustness when addressing the nonlinear filtering problems in the context of hydrological modeling(Clark et al., 2008; Moradkhani, Sorooshian, et al., 2005; Reichle, McLaughlin, & Entekhabi, 2002; Xie & Zhang, 2010).

Another well-known nonlinear extension to the KF is the unscented KF (UKF) (Julier et al., 1995). Its usefulness in nonlinear systems and efficient sampling strategy have led to extensive applications in many branches of science and engineering (Chatzi & Smyth, 2009; Chowdhary & Jategaonkar, 2010; Kandepu et al., 2008; St-Pierre & Gingras, 2004; Wu & Smyth, 2007). However, so far, the UKF has received little attention in the context of hydrological modeling (Liu et al., 2012a). A preliminary application shows its usefulness in state estimation by applying it to the Xinanjiang rainfall-runoff model (Jiang et al., 2018).

In this paper, we strive to investigate the application of UKF and EnKF to improve the forecast performance of a lowland hydrological model by updating the model state by assimilating streamflow measurements. We seek here to (1) introduce the basic theory of UKF and EnKF, (2) discuss the main differences and connections between UKF and EnKF, (3) demonstrate the usefulness of UKF in improving the forecast performance by estimating the state, and (4) compare the performance of UKF and EnKF in the context of flood forecasting.

2. Materials and Methods

2.1. State-Space Representation

A general framework for sequential data assimilation techniques is the state-space representation

$$\mathbf{X}_{k+1} = f(\mathbf{X}_k, \mathbf{U}_k, \mathbf{W}, \mathbf{V}_k) \tag{1}$$

$$\mathbf{Y}_{k+1} = h(\mathbf{X}_{k+1}, \mathbf{W}, \mathbf{n}_{k+1}) \tag{2}$$

where $\mathbf{X}_k$ is the state at time k, $\mathbf{U}_k$ is the forcing input, $\mathbf{W}$ is the set of model parameters, $\mathbf{V}_k$ is the process noise with the covariance matrix $\mathbf{Q}_k$, $\mathbf{Y}_{k+1}$ is the measurement at time $k+1$, $\mathbf{n}_{k+1}$ is the observation noise with the covariance matrix $\mathbf{R}_{k+1}$, $f(\cdot)$ represents the state transition function, and $h(\cdot)$ represents the measurement function. For simplicity, the process noise and observation noise are assumed to be additive and zero mean. Also, we only focus on state estimation in this study. So the above model can be rewritten as

$$\mathbf{X}_{k+1} = f(\mathbf{X}_k, \mathbf{U}_k) + \mathbf{V}_k \tag{3}$$

$$\mathbf{Y}_{k+1} = h(\mathbf{X}_{k+1}) + \mathbf{n}_{k+1} \tag{4}$$

KF is restricted to provide a recursive solution to the discrete-data linear filtering problem (i.e., $f(\cdot)$ and $h(\cdot)$ are linear models). For nonlinear cases such as the state estimation of nonlinear systems, nonlinear filters such as EnKF and UKF are used to provide the solution.

2.2. EnKF

EnKF is a Monte Carlo-based nonlinear filter (Gillijns et al., 2006). The approximation of error covariance is achieved by propagating an ensemble via the system. The updated ensemble members (n members) at time k ($\widehat{\chi}_k^i$, $i = 1, ..., n$) are propagated through the state transition function

$$\widehat{\chi}_{k+1}^{i-} = f\left(\widehat{\chi}_k^i, \mathbf{U}_k^i, \mathbf{V}_k^i\right), \qquad i = 1, ..., n \tag{5}$$

where $\widehat{\chi}_{k+1}^{i-}$ is the prediction of the ith ensemble member, $\mathbf{V}_k^i$ is the process noise which is assumed to be zero-mean white Gaussian noise, and $\mathbf{U}_k^i$ is the perturbed forcing data. Using the predicted ensemble members, one can obtain the error covariance matrix

$$\mathbf{P}_{k+1} = \frac{1}{n-1}\mathbf{E}_{k+1}\mathbf{E}_{k+1}^T \tag{6}$$

with the expectation of the error in each ensemble member

$$\mathbf{E}_{k+1} = \left[\widehat{\chi}_{k+1}^{1-} - \overline{\mathbf{X}}_{k+1}, ..., \widehat{\chi}_{k+1}^{n-} - \overline{\mathbf{X}}_{k+1}\right] \tag{7}$$

where $\overline{\mathbf{X}}_{k+1}$ is the ensemble mean obtained by

$$\overline{\mathbf{X}}_{k+1} = \frac{1}{n}\sum_{i=1}^{n}\widehat{\chi}_{k+1}^{i-} \tag{8}$$

Similarly, the predicted ensemble members $\widehat{\chi}_{k+1}^{i-}$ ($i = 1, ..., n$) are propagated via the measurement function

$$\widehat{\gamma}_{k+1}^{i-} = h\left(\widehat{\chi}_{k+1}^{i-}\right) \tag{9}$$

Then the ensemble mean is obtained by

$$\overline{\mathbf{Y}}_{k+1} = \frac{1}{n}\sum_{i=1}^{n}\widehat{\gamma}_{k+1}^{i-} \tag{10}$$

The Kalman gain is defined as

$$\mathbf{K}_{k+1} = \mathbf{P}_{k+1}\mathbf{H}\left(\mathbf{H}^T\mathbf{P}_{k+1}\mathbf{H} + \mathbf{R}_{k+1}\right)^{-1} \tag{11}$$

Practically, the two terms $\mathbf{P}_{k+1}\mathbf{H}$ and $\mathbf{H}^T\mathbf{P}_{k+1}\mathbf{H}$ in Equation 11 can be calculated by the following equations (Houtekamer & Mitchell, 2001):

$$\mathbf{P}_{k+1}\mathbf{H} = \frac{1}{n-1}\sum_{i=1}^{n}\left(\widehat{\chi}_{k+1}^{i-} - \overline{\mathbf{X}}_{k+1}\right)\left(\widehat{\gamma}_{k+1}^{i-} - \overline{\mathbf{Y}}_{k+1}\right)^T \tag{12}$$

and

$$\mathbf{H}^T\mathbf{P}_{k+1}\mathbf{H} = \frac{1}{n-1}\sum_{i=1}^{n}\left(\hat{\gamma}^{i\,-}_{k+1} - \overline{\mathbf{Y}}_{k+1}\right)\left(\hat{\gamma}^{i\,-}_{k+1} - \overline{\mathbf{Y}}_{k+1}\right)^T \tag{13}$$

To facilitate the comparison between UKF and EnKF, we rewrite the above equations (Equations 11–13):

$$\mathbf{K}_{k+1} = \mathbf{P}_{\mathbf{X}_{k+1}\mathbf{Y}_{k+1}}\mathbf{P}^{-1}_{\mathbf{Y}_{k+1}\mathbf{Y}_{k+1}} \tag{14}$$

with

$$\mathbf{P}_{\mathbf{X}_{k+1}\mathbf{Y}_{k+1}} = \frac{1}{n-1}\sum_{i=1}^{n}\left(\hat{\chi}^{i\,-}_{k+1} - \overline{\mathbf{X}}_{k+1}\right)\left(\hat{\gamma}^{i\,-}_{k+1} - \overline{\mathbf{Y}}_{k+1}\right)^T \tag{15}$$

and

$$\mathbf{P}_{\mathbf{Y}_{k+1}\mathbf{Y}_{k+1}} = \frac{1}{n-1}\sum_{i=1}^{n}\left(\hat{\gamma}^{i\,-}_{k+1} - \overline{\mathbf{Y}}_{k+1}\right)\left(\hat{\gamma}^{i\,-}_{k+1} - \overline{\mathbf{Y}}_{k+1}\right)^T \tag{16}$$

Using the Kalman gain, one can update the state of the ensemble members

$$\hat{\chi}^{i}_{k+1} = \hat{\chi}^{i\,-}_{k+1} + \mathbf{K}_{k+1}\left(\mathbf{Y}^{i}_{k+1} - \hat{\gamma}^{i\,-}_{k+1}\right) \tag{17}$$

with the perturbed observations

$$Y^{i}_{k+1} = Y_{k+1} + \eta^{i}_{k+1}, \quad \eta^{i}_{k+1} \sim N(0, R_{k+1}) \tag{18}$$

For more information about EnKF, we recommend Evensen (2003); Gillijns et al. (2006); Houtekamer and Mitchell (2001); Moradkhani, Sorooshian, et al. (2005); and Weerts and el Serafy (2006).

2.3. UKF

UKF is a nonlinear extension of KF to overcome the drawbacks of EKF, such as the obstacles when calculating the Jacobian matrix and the stability problem when the nonlinearity of the system is high. UKF utilizes a set of sample points (weighted sigma points) to propagate and capture the expected value and covariance (Julier et al., 2000). Various algorithms can be utilized by UKF to generate the sigma points, including the symmetric point algorithm, the minimal skew simplex point algorithm, and the spherical simplex point algorithm. The main distinction is the number of sigma points (hence the weights) used by the algorithm. For an L-dimensional state (space), the symmetric point algorithm requires $2L + 1$ sigma points, while the minimal skew simplex point algorithm requires $L + 1$ sigma points(Julier, 2003). However, for the minimal skew simplex point algorithm, problems of numerical instability can arise due to the radius bounding the sphere of the points. A general framework (scaled unscented transformation) is proposed to scale the sigma points when the dimension increases (Julier, 2002). The primary purpose of this study is to estimate the state of a conceptual hydrological model with four state variables, and hence the computational cost is low. The symmetric sampling strategy under the scaled framework is used to ensure the robustness of the system in this study.

All of the sample points are assigned with equal weight except the central point

$$W^{(c)}_{i} = W^{(m)}_{i} = 1/[2(L+\lambda)] \qquad i = 1,\ \ 2,\ ...,\ 2L \tag{19}$$

with the scaling parameter calculated by

$$\lambda = \alpha^2(L+\kappa) - L \tag{20}$$

where L is the number of the state variables ($L = 4$ in this study) and κ is a secondary scaling parameter. The weights for the central points are given as

$$W^{(c)}_{0} = \lambda/[(L+\lambda)] + 1 - \alpha^2 + \beta \tag{21}$$

and

$$W_0^{(m)} = \lambda/[(L+\lambda)] \tag{22}$$

where β can be adjusted to incorporate prior knowledge of the distribution of the state (e.g., β is set to 2 for Gaussian distribution). It is recommended that κ is set to $3 - L$ and α is set to a small positive value ($1 \geq \alpha \geq 10^{-4}$) to control the spread of sigma points around the mean. Note that only when all of the weights are nonnegative, it is guaranteed that the algorithm gives a positive semidefinite covariance. Therefore, such a choice of κ and α may lead to a nonpositive semidefinite covariance when the state dimension is higher than three and α is small. To avoid the potential problem, κ is set to 1 and α is set to 0.9 in this study.

For each iteration, a matrix with $2L + 1$ vectors (columns) of sigma points is obtained by

$$\widehat{\chi}_k = \left[\widehat{\mathbf{X}}_k \;\; \widehat{\mathbf{X}}_k + \gamma\sqrt{\mathbf{P}_k} \;\; \widehat{\mathbf{X}}_k - \left(\gamma\sqrt{\mathbf{P}_k}\right)\right] \tag{23}$$

with the

$$\gamma = \sqrt{(L+\lambda)} \tag{24}$$

where $\widehat{\mathbf{X}}_k$ is the estimated state at time k, $\mathbf{P}_k$ is the error covariance matrix, and $\sqrt{\mathbf{P}_k}$ is the matrix square root calculated by the Cholesky decomposition. $\widehat{\chi}_k$ is propagated through the state transition function

$$\widehat{\chi}^{*-}_{k+1} = f(\widehat{\chi}_k, \mathbf{U}_k) \tag{25}$$

Using the weights of the sigma points, one can obtain the mean and covariance

$$\widehat{\mathbf{X}}^-_{k+1} = \sum_{i=0}^{2L} W_i^{(m)} \widehat{\chi}^{*i\,-}_{k+1} \tag{26}$$

$$\mathbf{P}^-_{k+1} = \sum_{i=0}^{2L} W_i^{(c)} \left[\widehat{\chi}^{*i\,-}_{k+1} - \widehat{\mathbf{X}}^-_{k+1}\right]\left[\widehat{\chi}^{*i\,-}_{k+1} - \widehat{\mathbf{X}}^-_{k+1}\right]^T + \mathbf{Q} \tag{27}$$

where $\widehat{\chi}^{*i\,-}_{k+1}$ represents the ith column of $\widehat{\chi}^{*-}_{k+1}$ and $\mathbf{Q}$ represents the process-noise covariance, which is assumed to be constant for UKF in this study. To incorporate the process noise, one can resample the sigma points or expand the vector of the sigma points (Haykin, 2001). We will distinguish this new set of sigma points from the previous one by calling it $\widehat{\chi}^-_{k+1}$ (hence $\widehat{\chi}^{i\,-}_{k+1}$). Again, $\widehat{\chi}^-_{k+1}$ is propagated through the measurement model

$$\widehat{\gamma}^-_{k+1} = h\left(\widehat{\chi}^-_{k+1}\right) \tag{28}$$

Similarly, we can obtain the expected value

$$\widehat{\mathbf{Y}}^-_{k+1} = \sum_{i=0}^{2L} W_i^{(m)} \widehat{\gamma}^{i\,-}_{k+1} \tag{29}$$

With the measurement $\mathbf{Y}_{k+1}$ (without the additional perturbations as required by EnKF), the state is updated by

$$\widehat{\mathbf{X}}_{k+1} = \widehat{\mathbf{X}}^-_{k+1} + \mathbf{K}_{k+1}\left(\mathbf{Y}_{k+1} - \widehat{\mathbf{Y}}^-_{k+1}\right) \tag{30}$$

The Kalman gain is defined as

$$\mathbf{K}_{k+1} = \mathbf{P}_{\mathbf{X}_{k+1}\mathbf{Y}_{k+1}} \mathbf{P}^{-1}_{\mathbf{Y}_{k+1}\mathbf{Y}_{k+1}} \tag{31}$$

with

$$\mathbf{P}_{\mathbf{X}_{k+1}\mathbf{Y}_{k+1}} = \sum_{i=0}^{2L} W_i^{(c)} \left[\widehat{\chi}^{i\,-}_{k+1} - \widehat{\mathbf{X}}^-_{k+1}\right]\left[\widehat{\gamma}^{i\,-}_{k+1} - \widehat{\mathbf{Y}}^-_{k+1}\right]^T \tag{32}$$

and

$$\mathbf{P}_{\mathbf{Y}_{k+1}\mathbf{Y}_{k+1}} = \sum_{i=0}^{2L} W_i^{(c)} \left[\widehat{\boldsymbol{\gamma}}_{k+1}^{i-} - \widehat{\mathbf{Y}}_{k+1}^{-}\right] \left[\widehat{\boldsymbol{\gamma}}_{k+1}^{i-} - \widehat{\mathbf{Y}}_{k+1}^{-}\right]^T + \mathbf{R} \tag{33}$$

where $\mathbf{R}$ represents the measurement noise assumed to be constant in this study. Finally, the error covariance is updated by

$$\mathbf{P}_{k+1} = \mathbf{P}_{k+1}^{-} - \mathbf{K}_{k+1}\mathbf{P}_{\mathbf{Y}_{k+1}\mathbf{Y}_{k+1}}\mathbf{K}_{k+1}{}^T \tag{34}$$

For detailed information about UKF, we recommend Haykin (2001); Julier (2002, 2003).

2.4. Comparison of EnKF and UKF

Both approaches belong to the class of sampling-based filter algorithms in that the samples are generated and propagated through the state-space model to approximate the error statistics, and the procedures of UKF and EnKF are quite similar (Roth et al., 2015), but we highlight the following essential differences.

Equation 23 shows that in contrast to the Monte Carlo sampling strategy used by EnKF, the sigma points of UKF are generated in a deterministic way. For each iteration, EnKF maintains the ensemble members, while UKF generates the sigma points from the estimated state $\widehat{\mathbf{X}}_k$ and error covariance $\mathbf{P}_k$ of the previous time step. Second, UKF and EnKF differ in the weights of the samples. For UKF, the weights are obtained by the equations from Equations 19–22, while each ensemble member of EnKF is equally weighted. Furthermore, as indicated by Equations 27 and 34, the error covariance of UKF is recursively calculated in the time update step and updated in the measurement update step, while EnKF directly calculates the error covariance from a set of ensemble members.

Roughly speaking, all the three differences mentioned above are associated with the sampling strategies used by the filters, and different sampling strategies can lead to different accuracy. In terms of Taylor series expansion, the approximations of UKF can achieve at least the second-order accuracy in the face of an arbitrary nonlinear function. Under the Gaussian assumption, the approximations can achieve at least the third-order accuracy (Haykin, 2001). A preliminary theoretical analysis shows that under the Gaussian assumption, EnKF can achieve at least the first-order accuracy (Luo & Moroz, 2009). Note that the analysis does not necessarily mean that UKF can practically achieve a better approximation (performance) over EnKF since, for EnKF, an increase in the ensemble size can lead to higher accuracy. However, the size of the sigma points of UKF is fixed. From the perspective of the sample size, the sample size of UKF is determined by the dimension N of the state vector and the sampling algorithm used by UKF ranging from $N+1$ to $2*N+1$ (Julier, 2002, 2003; Julier & Uhlmann, 1997), while for EnKF, there is no standard criterion for determining the ensemble size (Gillijns et al., 2006).

It should be noted that EnKF has the advantage of including different sources of uncertainties more easily compared to UKF. For every time step, the sigma points of UKF are generated in a determined method using the state of the hydrological model and the corresponding error covariance, indicating that UKF considers the uncertainty in the state as the dominant uncertainty of hydrological modeling. The method for generating the ensemble members of EnKF is more flexible than the method of UKF, which makes it easy to include different sources of uncertainties such as considering uncertainty in the model inputs and uncertainty in the model state simultaneously in the ensemble members (hence in the filtering process), while for UKF, it would be difficult to include other uncertainties of hydrological modeling (e.g., uncertainty in the model inputs).

3. Case Studies

3.1. Tools and Models

In this study, the WALRUS model is used to conduct the experiments. WALRUS model is a lumped rainfall-runoff lowland model developed by Brauer, Torfs, et al. (2014). WALRUS consists of a soil reservoir which consists of a vadose zone and a groundwater zone, a quickflow reservoir, and a surface water reservoir (Figure 1). d_V, d_G, h_Q, and h_S represent the state variables of WALRUS. W, β, and $d_{V,eq}$ are dependent variables. P, ET_{pot}, f_{XG}, and f_{XS} are the model inputs. ET_{act} and Q are the model outputs. P_S, P_V, P_Q, ET_V, ET_S, f_{GS}, and f_{QS} are internal fluxes. The remaining terms in Figure 1 represent the model parameters. Here we

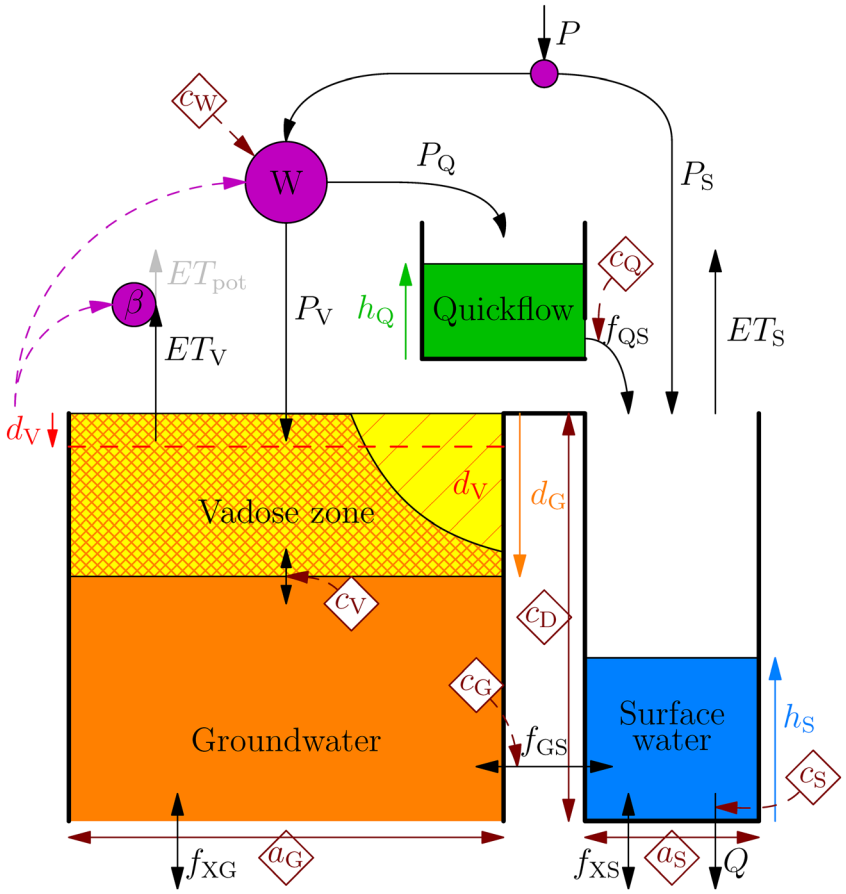

Figure 1. Flowchart of the model structure of WALRUS (Brauer, Torfs, et al., 2014).

only present a brief description of the state variables in Table 1. For detailed information about this model, we recommend Brauer, Torfs, et al. (2014) and Brauer, Teuling, et al. (2014).

The experiments were conducted within Delft-FEWS (Werner et al., 2013) using OpenDA-SOBEK. Delft-FEWS has its origin in flood forecasting and flood warning. In this study, Delft-FEWS is used to import data, run the forecasts, and export the results. The Delft-FEWS system used in this study (FEWS Vecht) is a standalone copy of the platform used by the water board for operational water management. OpenDA is a toolbox that is designed for data assimilation and calibration of numerical models (Rakovec et al., 2015). Both filtering algorithms used in this study (i.e., UKF and EnKF) have been included in OpenDA. SOBEK is a modeling software that mainly includes submodules for open water flow and rainfall-runoff processes in rural and urban environments, which can be used for flood forecasting, optimization of drainage systems, and control of irrigation systems. (Betrie et al., 2011; Bruni et al., 2015; Haile & Rientjes, 2005; Prinsen & Becker, 2011). WALRUS is available as a rainfall-runoff module (in C) within SOBEK. A wrapper for OpenDA-SOBEK-WALRUS is implemented to link the filter algorithms and the hydrological model.

3.2. Study Area and Data Basis

The Regge catchment is a lowland catchment in the east of the Netherlands, which covers an area of 957m^2 (Figure 2). The elevation differences are small, the soil is sandy, and land use is mostly grassland and agricultural. The catchment is freely draining, and although there is a broad canal flowing through the catchment, no surface water is expected to be exchanged between the canal and the catchment. The Regge catchment has been used in previous study using WALRUS (Heuvelink et al., 2020), so no calibration was required here. For WALRUS model, five parameters including c_W, c_V, c_G, c_Q, and c_S require calibration and two parameters including c_D and a_S are estimated from field observations. The values we used were

Table 1
Descriptions of the State Variables of WALRUS

Variable	Units	Description
d_V	mm	Storage deficit which is used to quantify the dryness of the vadose zone
d_G	mm	Ground depth which is used to compute the groundwater drainage flux
h_Q	mm	Quickflow reservoir level which is utilized to simulate the combined effect of all water through the quickflow path toward the surface water
h_S	mm	Surface water level with respect to the channel bottom

396 mm for c_W, 45 hr for c_V, 16×10^6 mm hr for c_G, 7.5 hr for c_Q, 0.2 mm hr^{-1} for c_S, 2,450 mm for c_D, and 0.01 for a_S. Loamy sand is used as the soil type.

The forcing data, precipitation, and potential evapotranspiration have been acquired from the Royal Netherlands Meteorological Institute (KNMI). Precipitation was measured at weather station Twenthe, and potential evapotranspiration was estimated using global radiation and temperature measured at the same station and the method of Makkink (Amatya et al., 1995; Winter et al., 1995; Xu & Singh, 2000). Discharge observations were used for both calibration and verification. The discharge was measured by the local water authority, Waterboard Vechtstromen. All data were provided with hourly resolution.

To improve the forecast performance, EnKF and UKF are used to estimate the model state by assimilating the observed discharge at the catchment outlet. In the first part of the experiment, both filters are operated every hour (i.e., with hourly time step) using the same size of ensemble members (nine ensemble members), while the forecasts are performed and issued every 2 days for the period ranging from 2000 to 2011. In the second part of the experiment, the performance of EnKF with different ensemble sizes (18 ensemble members, 36 ensemble members, and 72 ensemble members) is further evaluated. Due to the high computational cost, the second part covers a run of 1 year. In the study, both the forecast performance and the behavior of the updated model state are analyzed. Note that all the forecasts are obtained with the measured precipitation. Figure 3 displays a complete picture of the update-forecast procedure used by both UKF and EnKF.

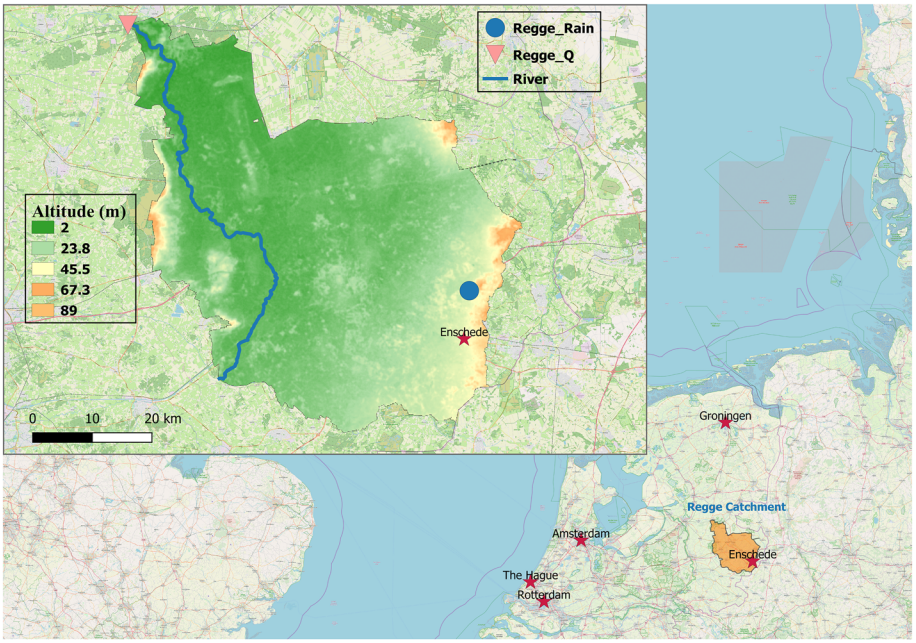

Figure 2. Map showing the location of the Regge catchment with the meteorological station and discharge measurement station. "Regge_Rain" represents the meteorological station, and "Regge_Q" represents the discharge measurement station.

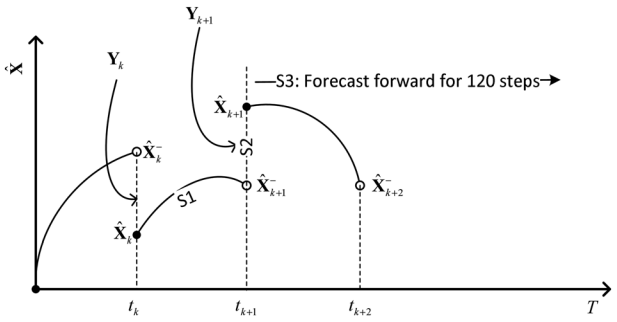

Figure 3. A complete picture of the update-forecast procedure. The horizontal axis represents the time, and the vertical axis stands for the predicted state and updated state. Assume that t_{k+1} is the current time, and the update-forecast procedure is as follows: The state prediction at time t_{k+1} is obtained by running the hydrological model with the updated state at time t_k ($\widehat{\mathbf{X}}_k$) (Step 1, S1). Then the updated state at time t_{k+1} ($\widehat{\mathbf{X}}_{k+1}$) is obtained by updating the state prediction $\widehat{\mathbf{X}}_{k+1}^-$ using the streamflow observation at time ($\mathbf{Y}_{k+1}$) (Step 2, S2). Finally, issue the forecast by running the hydrological model with the updated state at time t_{k+1} ($\widehat{\mathbf{X}}_{k+1}$) with the measured precipitation for 120 steps (Step 3, S3).

In this study, the ensemble members of EnKF are obtained by perturbing the forcing data (i.e., precipitation) (Moradkhani, Sorooshian, et al., 2005). The multiplicative noise to perturb the precipitation data is assumed to be lognormal distributed with the standard deviation equal to 0.25. Perturbations to the discharge observations are assumed to be similar to the multiplicative noise setting used by Weerts and el Serafy (2006) with a standard deviation equal to 0.05 times the observed discharge. For UKF, since there is no prior information about the noise of this practical problem such as the noise magnitude, the noise covariance for UKF is assumed to be constant and set empirically. The measurement-noise covariance is set equal to 0.05, and the process-noise covariance is assumed to be a diagonal matrix $\mathbf{Q} = \text{diag}(0.5,0.5,0.5,0.5)$.

The Ensemble Verification System (EVS) is used to evaluate the performance of flood forecasting methods, including ensemble forecasts such as streamflow and precipitation (Brown et al., 2010). While many metrics have been included in EVS, in this study, we consider the root mean squared error (*RMSE*), the mean absolute error (*MAE*), and the continuous ranked probability score (*CRPS*) for evaluating the forecast performance. *RMSE* and *MAE* are used to evaluate the single-valued forecast performance (i.e., UKF and the ensemble mean of EnKF) since UKF is designed to provide a single-valued result, while *CRPS* is used to evaluate the performance of ensemble forecasts of EnKF. One advantage of the *CRPS* is that it reduces to the *MAE* if the forecast is deterministic, which makes it possible to compare an ensemble forecast with a deterministic forecast (Hersbach, 2000). In brief, a perfect match of the model outputs to the measurements has a value of zero. For detailed information about the metrics, we refer to Hersbach (2000), Brown et al. (2010), Wilks (2011), and Verkade et al. (2013).

4. Results and Discussion

4.1. Effect of UKF and EnKF on Forecast Performance

Figure 4 shows a plot of the output forecast performance of UKF and the ensemble mean of EnKF measured by *RMSE* when increasing the lead time from 1 to 120 hr.

Note that for clarity, we only show the results for all the data, "top 10%," and "top 25%," as the results were similar for "top 50%" and "top 75%." The results for "top 50%" and "top 75%" can be found in the supporting information (Figure S1). Figure 4 shows that both UKF and EnKF can significantly improve the forecast performance since the *RMSE* of UKF and EnKF considerably lower as compared with the corresponding *RMSE* of WALRUS. UKF has achieved better performance when the lead time ranging from 1 to 60 hr since the values obtained by UKF are lower than the values of EnKF. The difference between the updated performance (either obtained by UKF or EnKF) and the original performance suggests that both filtering algorithms can improve the forecast performance by updating the model state (hence altering the model behavior). Besides, the difference between the improvements in the forecast performance (i.e., the difference between the improvement of EnKF and the improvement of UKF) tends to decrease when increasing the lead time.

Figure 5 shows a similar plot to Figure 4 (measured by *MAE* and *CRPS*). Note that *CRPS* is reduced to *MAE* when the forecast is deterministic. Hence, *CRPS* is used to evaluate the performance of all the ensemble members of EnKF, while *MAE* is used to evaluate the performance of the ensemble mean of EnKF and UKF. As expected, both UKF and EnKF have improved the forecast performance, and there is a general trend for the forecast performance to decrease when increasing the lead time. Note that there is a slight difference between the *CRPS* of the ensemble members of EnKF and the *MAE* of the ensemble mean of EnKF, and the difference tends to increase with lead time. The above observation may suggest that the advantages of ensemble forecasts (with respect to the ensemble mean) increase for longer lead times when using EnKF. Besides, as illustrated by Figures 4 and 5 (especially in Figure 5), EnKF outperforms UKF for the top 10% high flow when the lead time is greater than 85 hr.

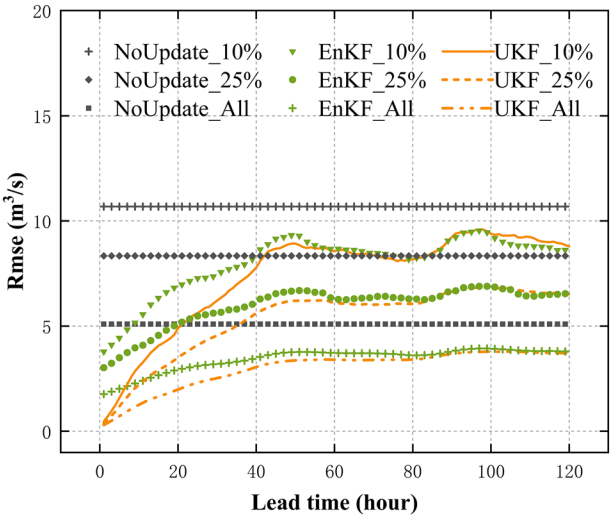

Figure 4. Forecast performance of UKF ("UKF_All," "UKF_10%," and "UKF_25%"), the mean of the ensemble members of EnKF ("EnKF_All," "EnKF_10%," and "EnKF_25%"), and WALRUS model without updating ("NoUpdate_All," "NoUpdate_10%," and "NoUpdate_25%") measured by *RMSE*. It is assumed that the subsets of outputs corresponding to the 10% highest observations and 25% highest observations result in the sets suffixed by "_10%" and "_25%," respectively. Also, all the outputs result in the set suffixed by "_All."

It should be noted that the better performance of UKF in this study does not necessarily mean that UKF is better than EnKF since the experiment in this study is conducted in a practical and nearly operational context where a fair comparison between the two approaches can be hampered by many factors such as the difference in the strategies for noise specification of both filters. EnKF used in this study incorporates the noise information by randomly perturbing the ensembles, as indicated by Equations 5 and 18, while UKF used in this study incorporates the noise information by directly adding the covariance matrix of the noise to the error covariance matrix (Equations 27 and 33). In addition, both filters set up the noise information empirically (especially for UKF), although similar noise specification strategies of EnKF have been used in the literature (Moradkhani, Sorooshian, et al., 2005; Weerts & el Serafy, 2006). The noise setting of UKF used in this study is simpler as compared with the noise setting of EnKF. The covariance of the measurement noise is set to a smaller value compared with the one of the process noise, indicating that the filter tends to have "more trust" in the measured values than the simulated values. This also contributes to the high accuracy of the updated output and the forecast output of UKF at short lead times. It may be possible and preferable to adaptively adjust the noise settings at each step of the filter (Clark et al., 2008; Drécourt et al., 2006; Noh et al., 2014; Wang & Bai, 2008); however, this is deemed beyond the scope of this study. At least, the results of this study are encouraging and suggesting that UKF can become an effective and robust method to assimilate observations into low-dimensional models.

4.2. Behaviors of Updated Model Output and Model State

Figure 6 shows the updated outputs of four typical flood events. Both filters have increased the performance of the outputs by updating the model state.

We further analyze the updated states and outputs based on the flood event from 1 August 2006, 01:00:00 to 8 August 2006, 01:00:00 (the flood event located in the bottom right of Figure 6). Figure 7 shows the trajectories of updated states for the flood event. For clarity, in Figure 7, we only show the mean of the ensemble members rather than all the ensemble members.

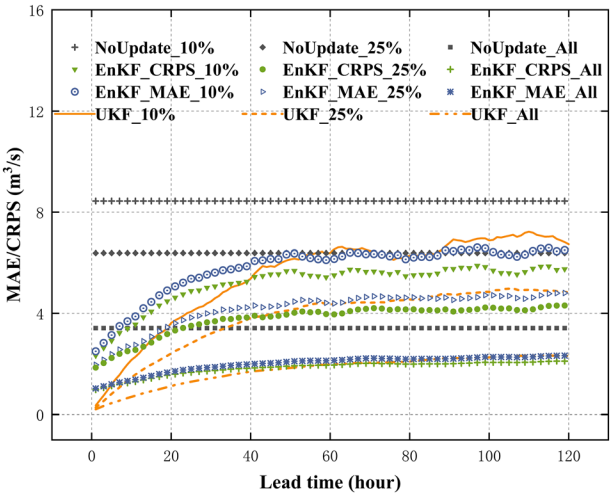

Figure 5. Forecast performance of UKF measured by *MAE* ("UKF_All," "UKF_10%," and "UKF_25%"), the mean of the ensemble members of EnKF measured by *MAE* ("EnKF_MAE_All," "EnKF_MAE_10%," and "EnKF_MAE_25%"), the ensemble members of EnKF measured by *CRPS* ("EnKF_CRPS_All," "EnKF_ CRPS_10%," and "EnKF_CRPS_25%"), and WALRUS model without updating measured by *MAE* ("NoUpdate_All," "NoUpdate_10%," and "NoUpdate_25%").

As expected, both UKF and EnKF can significantly improve the performance of outputs when the original model performance without updating is not satisfactory. The original performance may be caused by a poor initial condition in the model state.

Figure 7 shows that for both updated scenarios (UKF and EnKF), compared with the trend of the original state ("NoUpdate"), the trends (behaviors) of h_S and h_Q have been adjusted significantly during the flood event and are consistent with the corresponding trends of the updated model output. To further analyze the model behaviors using UKF and EnKF, we present the equations (Brauer, Torfs, et al., 2014)

$$d_G = \mathrm{f}(d_V) \tag{35}$$

$$f_{QS} = \mathrm{f}_0(h_Q) \tag{36}$$

$$f_{GS} = \mathrm{f}_1(h_S, d_G) \tag{37}$$

$$\frac{dh_s}{dt} = \mathrm{f}_2\left(f_{QS} + f_{XS} + f_{GS}\right) \tag{38}$$

$$Q = \mathrm{f}_3(h_S) \tag{39}$$

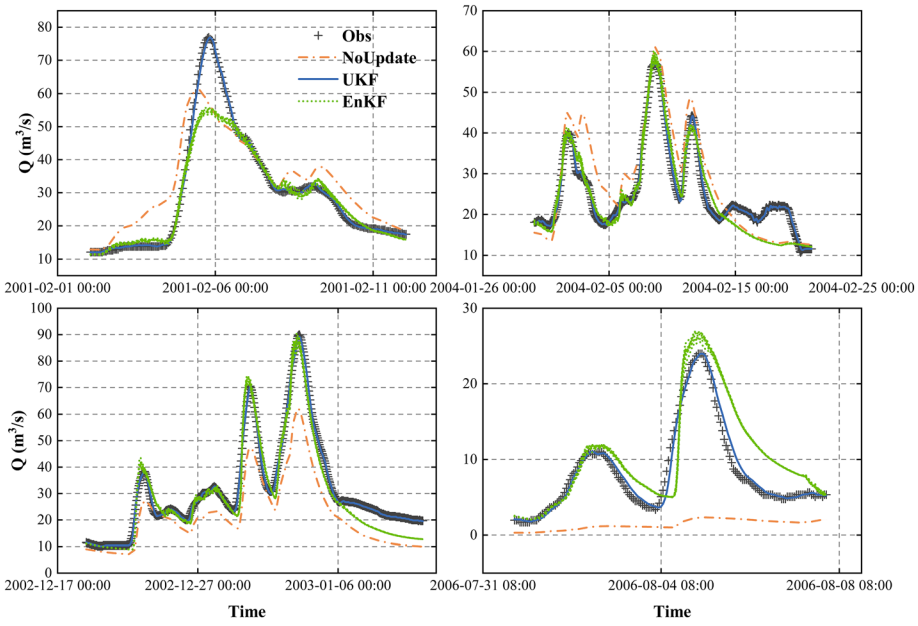

Figure 6. Updated discharge of four typical flood events at the catchment outlet obtained by EnKF and UKF: "NoUpdate" and "Obs" represent the outputs of the WALRUS model and the observed discharge, respectively.

where d_V represents the storage deficit, d_G represents the groundwater depth, h_Q represents the quickflow reservoir level, f_{QS} represents the quickflow, h_S represents the surface water level, f_{GS} represents the groundwater drainage/surface water infiltration, f_{XS} represents the external flow for surface water (not included in this case), and Q represents the model output. For simplicity, the actual functions of WALRUS model are represented by f, f_0, f_1, f_2, and f_3. The model parameters, inputs (e.g., precipitation), and outputs (e.g., actual evapotranspiration) are also omitted in these equations. Equation 39 indicates the model output Q is a single function of h_S, and hence it can be expected that for each scenario (UKF, EnKF, or WALRUS), the trajectory of h_S is almost identical with the trajectory of Q. Note that time series f_{XS} should be provided by the user (Brauer, Torfs, et al., 2014). In this study, for simplicity, it is assumed to be zero. Therefore, it makes sense that the filters may attribute the effect of the external flow to the other independent variables f_{QS} and f_{GS} (Equation 38). Together with Equations 36 and 37, it can be expected that the filters will adjust all the state variables, while for all the scenarios (WALRUS, UKF, and EnKF), the trends of d_V and d_G are similar. The reason for this is that the groundwater depth d_G tends to remain unchanged since the model structure determines that d_G does not respond quickly to rainfall (Brauer, Teuling, et al., 2014). Also, d_G is not an independent variable but tends to an equilibrium value of d_V.Hence, both filters tend to change the trends of h_S and h_Q during the flood event. This suggests that the updated behaviors can be affected by the model structure. Therefore, UKF and EnKF have behaved in a similar manner.

Note that the observed discharge starts to increase before the precipitation appears. This inconsistency between the precipitation and the observed discharge may be caused by the spatial distribution of precipitation over the study area since we only use the precipitation data from the Twenthe station, which is located in the east of Regge catchment. Considering the inconsistency in the observed data, both filters may have steered the model states in a wrong direction, though satisfactory performance has been obtained by both approaches.

4.3. Effect of Increasing Ensemble Members of EnKF on Forecast Performance

Figure 8 displays the performance of EnKF with different numbers of ensemble members as measured by *RMSE* (1 year run from 2000 to 2001).

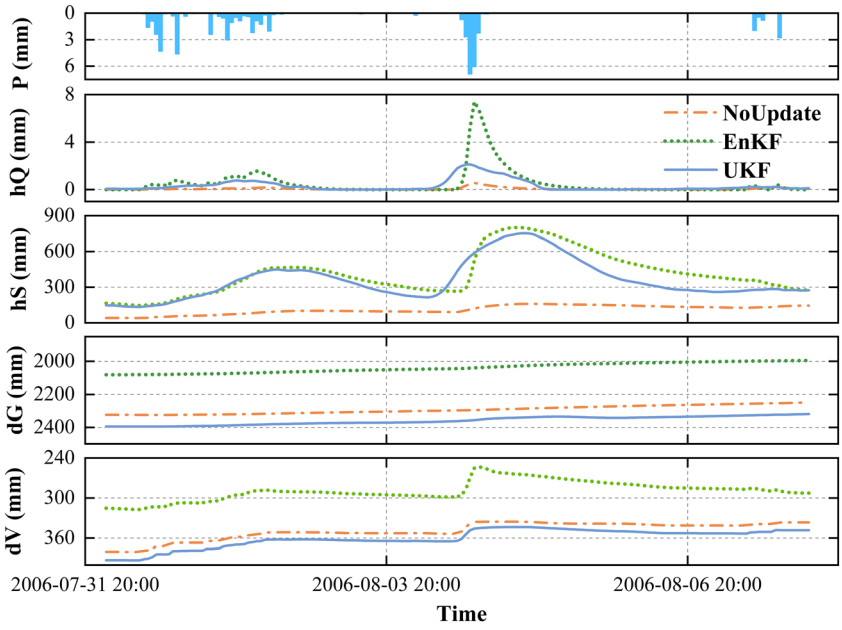

Figure 7. Updated state variables (h_S, h_Q, h_S, and d_V, see Table 1) for the flood event from 1 August 2006, 01:00:00 to 8 August 2006, 01:00:00.

As expected, there is a slight decrease in *RMSE* when increasing the size of ensemble members from 9 to 18, indicating an increase in the forecast performance. However, it can also be observed that the performance of EnKF with even more ensemble members (i.e., 36 ensemble members and 72 ensemble members) is almost the same as the performance of EnKF using 18 ensemble members. This observation indicates that an increase in the size of the ensemble members does not necessarily mean a further improvement in the performance. A preliminary analysis of other studies shows similar results about the relationship between the size of ensemble members used by EnKF and the performance (Gillijns et al., 2006; Rakovec et al., 2015).

5. Conclusions

In this study, the UKF and the EnKF are employed to improve the forecast skill of a lowland conceptual hydrologic model by state estimation. In the context of hydrological modeling, EnKF is a widely used data assimilation technique, while UKF has received little attention. Both filters were tested with a reforecast experiment in an operational context using an hourly time step. In this study, we first operated EnKF and UKF with nine ensemble members for 10 years reforecast period using perfect rainfall. The results show that both UKF and EnKF can improve the forecast performance significantly for all the lead times. With the same number of ensemble members, UKF has achieved better performance. The analysis of a flood event selected from the experiment period shows that both UKF and EnKF adjust the model state in similar behavior to react to flow processes.

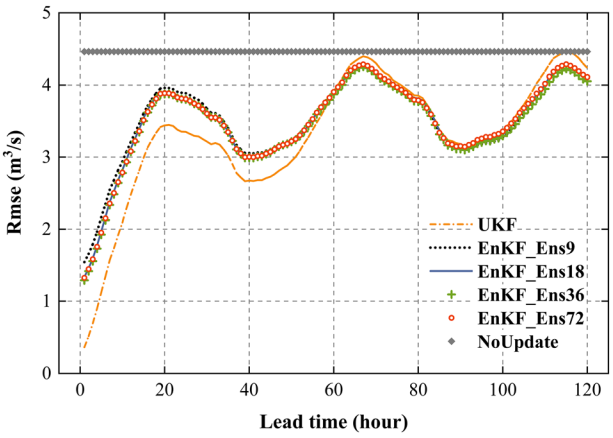

Figure 8. Forecast performance of UKF and EnKF with different sizes of ensemble members measured by *RMSE* (all data): It is assumed that the subsets of EnKF using m ensemble members result in sets suffixed by "_Ens$m$" (i.e., "EnKF_Ens9" represents the results using nine ensemble members).

When using EnKF, one must be concerned with the fact that the ensemble size can influence the performance of the filter. Hence, we also investigated the performance of EnKF with more ensemble members (18 ensemble members, 36 ensemble members, and 72 ensemble members). The results show that an increase in the size of the ensemble members does not necessarily mean a significant increase in the performance. Hence, it is necessary to consider the tradeoff between the performance and the computational cost. The results of this study suggest that UKF can be an effective and useful method to assimilate the observed discharge into

low-dimensional models in the context of operational flood forecasting. Note that UKF is designed to handle low-dimension problems. Therefore, one may still prefer to use EnKF when the dimension of the system is higher.

It is worth noting that uncertainty may stem from several sources, such as model structure, model parameters, model states, and initial conditions (Clark & Vrugt, 2006; Kuczera et al., 2006; Sun, Bao, Jiang, Ji, et al., 2018). However, in this study, we only update the model state, indicating all the uncertainties are attributed to state uncertainty, which may result in model states being twisted but a satisfactory performance from the perspective of the model residual (Sun, Bao, Jiang, Si, et al., 2018). Therefore, future work is needed to take other uncertainties into account, such as extending the state estimation to the joint state parameter estimation, which considers the uncertainties of model state and model parameters simultaneously. Another limitation of this study is the relatively simple noise specification strategies for both filters, especially for UKF; the measurement noise and the process noise are set to constant values empirically. Hence, more investigations on the strategies for noise specification and their effects on forecast accuracy deserve more attention in future studies.

Data Availability Statement

All data used in this paper are available online, and the link to download the data is as follows: https://data.4tu.nl/repository/uuid:dfe80f20-2031-4d0c-a7f5-82a840248c20.

Acknowledgments

We thank Deltares for providing the software and models. The areal averaged hourly data, including the precipitation and potential evapotranspiration for Regge catchment, were provided by the Royal Netherlands Meteorological Institute (KNMI). The measured discharge data were provided by the Water Board Vechtstromen. We thank these organizations for granting permission to use their data. We thank Geert Prinsen for the help with WALRUS (Deltares). We thank Klaas-Jan van Heeringen and Erik Pelgrim for their help with connecting the OpenDA with Sobek (both from Deltares). Bart van Osnabrugge (Deltares), Bob van Rongen (Deltares), and Vinicius Siqueira (IPH/UFRGS, Brazil) are also thanked for the discussions. This research was supported by China Scholarship Council, the Postgraduate Research & Practice Innovation Program of Jiangsu Province (KYCX18_0575), the Fundamental Research Funds for Central Universities (2018B604X14), the National Key R&D Program of China (2016YFC0402703), and the National Natural Science Foundation of China (Grant Nos. 51709077, 51709076, 51479062, and 41371048).

References

Ajami, N. K., Duan, Q., & Sorooshian, S. (2007). An integrated hydrologic Bayesian multimodel combination framework: Confronting input, parameter, and model structural uncertainty in hydrologic prediction. *Water Resources Research*, *43*, W01403. https://doi.org/10.1029/2005WR004745

Amatya, D. M., Skaggs, R. W., & Gregory, J. D. (1995). Comparison of methods for estimating REF-ET. *Journal of Irrigation and Drainage Engineering*, *121*(6), 427–435. https://doi.org/10.1061/(ASCE)0733-9437(1995)121:6(427)

Arnold, J. G., Srinivasan, R., Muttiah, R. S., & Williams, J. R. (1998). Large area hydrologic modeling and assessment part I: Model development 1. *JAWRA Journal of the American Water Resources Association*, *34*(1), 73–89. https://doi.org/10.1111/j.1752-1688.1998.tb05961.x

Arulampalam, M. S., Maskell, S., Gordon, N., & Clapp, T. (2002). A tutorial on particle filters for online nonlinear/non-Gaussian Bayesian tracking. *IEEE Transactions on Signal Processing*, *50*(2), 174–188. https://doi.org/10.1109/78.978374

Betrie, G. D., Van Griensven, A., Mohamed, Y. A., Popescu, I., Mynett, A. E., & Hummel, S. (2011). Linking SWAT and SOBEK using open modeling interface (OPENMI) for sediment transport simulation in the Blue Nile River basin[J]. *Transactions of the ASABE*, *54*(5), 1749–1757.

Beven, K. (1993). Prophecy, reality and uncertainty in distributed hydrological modelling. *Advances in Water Resources*, *16*(1), 41–51. https://doi.org/10.1016/0309-1708(93)90028-E

Beven, K., & Binley, A. (1992). The future of distributed models: Model calibration and uncertainty prediction. *Hydrological Processes*, *6*(3), 279–298. https://doi.org/10.1002/hyp.3360060305

Brauer, C. C., Overeem, A., Leijnse, H., & Uijlenhoet, R. (2016). The effect of differences between rainfall measurement techniques on groundwater and discharge simulations in a lowland catchment. *Hydrological Processes*, *30*(21), 3885–3900. https://doi.org/10.1002/hyp.10898

Brauer, C. C., Teuling, A. J., Torfs, P. J. J. F., & Uijlenhoet, R. (2013). Investigating storage-discharge relations in a lowland catchment using hydrograph fitting, recession analysis, and soil moisture data. *Water Resources Research*, *49*, 4257–4264. https://doi.org/10.1002/wrcr.20320

Brauer, C. C., Teuling, A. J., Torfs, P. J. J. F., & Uijlenhoet, R. (2014). The Wageningen Lowland Runoff Simulator (WALRUS): A lumped rainfall-runoff model for catchments with shallow groundwater. *Geoscientific Model Development*, *7*(5), 2313–2332. https://doi.org/10.5194/gmd-7-2313-2014

Brauer, C. C., Torfs, P. J. J. F., Teuling, A. J., & Uijlenhoet, R. (2014). The Wageningen Lowland Runoff Simulator (WALRUS): Application to the Hupsel Brook catchment and the Cabauw polder. *Hydrology and Earth System Sciences*, *18*(10), 4007–4028. https://doi.org/10.5194/hess-18-4007-2014

Broersen, P. M., & Weerts, A. H. (2005). Automatic error correction of rainfall-runoff models in flood forecasting systems. Paper presented at the 2005 IEEE Instrumentation and Measurement Technology Conference Proceedings, Ottawa, Ont, Canada.

Brown, J. D., Demargne, J., Seo, D.-J., & Liu, Y. (2010). The Ensemble Verification System (EVS): A software tool for verifying ensemble forecasts of hydrometeorological and hydrologic variables at discrete locations. *Environmental Modelling & Software*, *25*(7), 854–872. https://doi.org/10.1016/j.envsoft.2010.01.009

Bruni, G., Reinoso, R., van de Giesen, N., Clemens, F., & ten Veldhuis, J. (2015). On the sensitivity of urban hydrodynamic modelling to rainfall spatial and temporal resolution. *Hydrology and Earth System Sciences*, *19*(2), 691–709. https://doi.org/10.5194/hess-19-691-2015

Burgers, G., Jan van Leeuwen, P., & Evensen, G. (1998). Analysis scheme in the ensemble Kalman filter. *Monthly Weather Review*, *126*(6), 1719–1724. https://doi.org/10.1175/1520-0493(1998)126%3C1719:ASITEK%3E2.0.CO;2

Butts, M. B., Payne, J. T., Kristensen, M., & Madsen, H. (2004). An evaluation of the impact of model structure on hydrological modelling uncertainty for streamflow simulation. *Journal of Hydrology*, *298*(1–4), 242–266. https://doi.org/10.1016/j.jhydrol.2004.03.042

Chatzi, E. N., & Smyth, A. W. (2009). The unscented Kalman filter and particle filter methods for nonlinear structural system identification with non-collocated heterogeneous sensing. *Structural Control and Health Monitoring*, *16*(1), 99–123. https://doi.org/10.1002/stc.290

Chowdhary, G., & Jategaonkar, R. (2010). Aerodynamic parameter estimation from flight data applying extended and unscented Kalman filter. *Aerospace Science and Technology*, *14*(2), 106–117. https://doi.org/10.1016/j.ast.2009.10.003

Clark, M. P., Rupp, D. E., Woods, R. A., Zheng, X., Ibbitt, R. P., Slater, A. G., et al. (2008). Hydrological data assimilation with the ensemble Kalman filter: Use of streamflow observations to update states in a distributed hydrological model. *Advances in Water Resources*, *31*(10), 1309–1324. https://doi.org/10.1016/j.advwatres.2008.06.005

Clark, M. P., & Vrugt, J. A. (2006). Unraveling uncertainties in hydrologic model calibration: Addressing the problem of compensatory parameters. *Geophysical Research Letters*, *33*, L06406. https://doi.org/10.1029/2005GL025604

Da Ros, D., & Borga, M. (1997). Adaptive use of a conceptual model for real time flood forecasting. *Hydrology Research*, *28*(3), 169–188. https://doi.org/10.2166/nh.1997.0010

Deltares. (2013). Deltares: SOBEK, 1D/2D Modeling Suite for Integral Water Solutions: Hydrodynamics, Rainfall Runoff and Real-Time Control, Deltares, Delft, available at: www.deltares.nl

Drécourt, J.-P., Madsen, H., & Rosbjerg, D. (2006). Calibration framework for a Kalman filter applied to a groundwater model. *Advances in Water Resources*, *29*(5), 719–734. https://doi.org/10.1016/j.advwatres.2005.07.007

Evensen, G. (1994). Sequential data assimilation with a nonlinear quasi-geostrophic model using Monte Carlo methods to forecast error statistics. *Journal of Geophysical Research*, *99*(C5), 10143–10,162. https://doi.org/10.1029/94JC00572

Evensen, G. (2003). The ensemble Kalman filter: Theoretical formulation and practical implementation. *Ocean Dynamics*, *53*(4), 343–367. https://doi.org/10.1007/s10236-003-0036-9

Francois, C., Quesney, A., & Ottlé, C. J. J. O. H. (2003). Sequential assimilation of ERS-1 SAR data into a coupled land surface-hydrological model using an extended Kalman filter. *Journal of Hydrometeorology*, *4*(2), 473–487.

Georgakakos, K. P. (1986). A generalized stochastic hydrometeorological model for flood and flash-flood forecasting: 1. Formulation. *Water Resources Research*, *22*(13), 2083–2095. https://doi.org/10.1029/WR022i013p02083

Gillijns, S., Mendoza, O. B., Chandrasekar, J., Moor, B. L. R. D., Bernstein, D. S., & Ridley, A. (2006). What is the ensemble Kalman filter and how well does it work? Paper presented at the 2006 American Control Conference, Minneapolis, MN, USA.

Gupta, H. V., Beven, K. J., & Wagener, T. (2006). Model calibration and uncertainty estimation. Encyclopedia of hydrological sciences.

Guse, B., Reusser, D. E., & Fohrer, N. (2013). How to improve the representation of hydrological processes in SWAT for a lowland catchment—Temporal analysis of parameter sensitivity and model performance. *Hydrological Processes*, *28*(4), 2651–2670.

Haile, A. T., & Rientjes, T. H. M. (2005). Effects of LIDAR DEM resolution in flood modelling : a model sensitivity study for the city of Tegucigalpa, Honduras. In M. G. Vosselman & C. Brenner (Eds.), *ISPRS 2005: Vol. XXXVI Comm. 3 W19 proceedings of the ISPRS workshop laser scanning 2005, 12-15 September, Enschede ITC The Netherlands / ed. by M.G. Vosselman and C. Brenner. Enschede : ITC* (6 p.). Enschede, The Netherlands.

Haykin, S. (2001). *Kalman filtering and neural networks* (Vol. 47). New Jersey: John Wiley & Sons. https://doi.org/10.1002/0471221546

Hersbach, H. (2000). Decomposition of the continuous ranked probability score for ensemble prediction systems. *Weather and Forecasting*, *15*(5), 559–570. https://doi.org/10.1175/1520-0434(2000)015%3C0559:DOTCRP%3E2.0.CO;2

Heuvelink, D., Berenguer, M., Brauer, C. C., & Uijlenhoet, R. (2020). Hydrological application of radar rainfall nowcasting in the Netherlands. *Environment International*, *136*, 105431. https://doi.org/10.1016/j.envint.2019.105431

Houtekamer, P. L., & Mitchell, H. L. (2001). A sequential ensemble Kalman filter for atmospheric data assimilation. *Monthly Weather Review*, *129*(1), 123–137. https://doi.org/10.1175/1520-0493(2001)129%3C0123:ASEKFF%3E2.0.CO;2

Jazwinski, A. H. (1970). *Stochastic processes and filtering theory*. New York: Elsevier.

Jiang, P., Sun, Y., & Bao, W. (2018). State estimation of conceptual hydrological models using unscented Kalman filter. *Hydrology Research*, *50*(2), 479–497.

Julier, S. J. (2002). The scaled unscented transformation. Paper presented at the American Control Conference, 2002. Proceedings of the 2002, Anchorage, AK, USA.

Julier, S. J. (2003). The spherical simplex unscented transformation. Paper presented at the American Control Conference, 2003. Proceedings of the 2003, Denver, CO, USA.

Julier, S. J., & Uhlmann, J. K. (1997). New extension of the Kalman filter to nonlinear systems. Paper presented at the Signal Processing, Sensor Fusion, and Target Recognition VI, Orlando, FL, USA.

Julier, S. J., Uhlmann, J. K., & Durrant-Whyte, H. F. (1995). A new approach for filtering nonlinear systems. Paper presented at the American Control Conference, Proceedings of the 1995, Seattle, WA, USA.

Julier, S. J., Uhlmann, J. K., & Durrant-Whyte, H. F. (2000). A new method for the nonlinear transformation of means and covariances in filters and estimators. *IEEE Transactions on Automatic Control*, *45*(3), 477–482. https://doi.org/10.1109/9.847726

Kalman, R. E. (1960). A new approach to linear filtering and prediction problems. *Journal of Basic Engineering*, *82*(1), 35–45. https://doi.org/10.1115/1.3662552

Kandepu, R., Foss, B., & Imsland, L. (2008). Applying the unscented Kalman filter for nonlinear state estimation. *Journal of Process Control*, *18*(7-8), 753–768. https://doi.org/10.1016/j.jprocont.2007.11.004

Kuczera, G., Kavetski, D., Franks, S., & Thyer, M. (2006). Towards a Bayesian total error analysis of conceptual rainfall-runoff models: Characterising model error using storm-dependent parameters. *Journal of Hydrology*, *331*(1-2), 161–177. https://doi.org/10.1016/j.jhydrol.2006.05.010

Kuczera, G., & Parent, E. (1998). Monte Carlo assessment of parameter uncertainty in conceptual catchment models: The Metropolis algorithm. *Journal of Hydrology*, *211*(1–4), 69–85. https://doi.org/10.1016/S0022-1694(98)00198-X

Li, Z., Shao, Q., Xu, Z., & Cai, X. (2010). Analysis of parameter uncertainty in semi-distributed hydrological models using bootstrap method: A case study of SWAT model applied to Yingluoxia watershed in northwest China. *Journal of Hydrology*, *385*(1–4), 76–83. https://doi.org/10.1016/j.jhydrol.2010.01.025

Lindström, G., Johansson, B., Persson, M., Gardelin, M., & Bergström, S. (1997). Development and test of the distributed HBV-96 hydrological model. *Journal of Hydrology*, *201*(1-4), 272–288. https://doi.org/10.1016/S0022-1694(97)00041-3

Liu, Y., & Gupta, H. V. (2007). Uncertainty in hydrologic modeling: Toward an integrated data assimilation framework. *Water Resources Research*, *43*, W07401. https://doi.org/10.1029/2006WR005756

Liu, Y., Weerts, A., Clark, M., Hendricks Franssen, H.-J., Kumar, S., Moradkhani, H., et al. (2012a). Advancing data assimilation in operational hydrologic forecasting: progresses, challenges, and emerging opportunities.

Liu, Y., Weerts, A. H., Clark, M., Hendricks Franssen, H. J., Kumar, S., Moradkhani, H., et al. (2012b). Advancing data assimilation in operational hydrologic forecasting: Progresses, challenges, and emerging opportunities. *Hydrology and Earth System Sciences*, *16*(10), 3863–3887. https://doi.org/10.5194/hess-16-3863-2012

Lü, H., Yu, Z., Zhu, Y., Drake, S., Hao, Z., & Sudicky, E. A. (2011). Dual state-parameter estimation of root zone soil moisture by optimal parameter estimation and extended Kalman filter data assimilation. *Advances in Water Resources*, *34*(3), 395–406. https://doi.org/10.1016/j.advwatres.2010.12.005

Luo, X., & Moroz, I. M. (2009). Ensemble Kalman filter with the unscented transform. *Physica D: Nonlinear Phenomena*, *238*(5), 549–562. https://doi.org/10.1016/j.physd.2008.12.003

McMillan, H., Jackson, B., Clark, M., Kavetski, D., & Woods, R. (2011). Rainfall uncertainty in hydrological modelling: An evaluation of multiplicative error models. *Journal of Hydrology*, *400*(1–2), 83–94. https://doi.org/10.1016/j.jhydrol.2011.01.026

Moradkhani, H., Hsu, K. L., Gupta, H., & Sorooshian, S. (2005). Uncertainty assessment of hydrologic model states and parameters: Sequential data assimilation using the particle filter. *Water Resources Research*, *41*, W05012. https://doi.org/10.1029/2004WR003604

Moradkhani, H., Sorooshian, S., Gupta, H. V., & Houser, P. R. (2005). Dual state-parameter estimation of hydrological models using ensemble Kalman filter. *Advances in Water Resources*, *28*(2), 135–147. https://doi.org/10.1016/j.advwatres.2004.09.002

Noh, S. J., Rakovec, O., Weerts, A. H., & Tachikawa, Y. (2014). On noise specification in data assimilation schemes for improved flood forecasting using distributed hydrological models. *Journal of Hydrology*, *519*, 2707–2721. https://doi.org/10.1016/j.jhydrol.2014.07.049

Prinsen, G. F., & Becker, B. P. J. (2011). Application of SOBEK hydraulic surface water models in the Netherlands Hydrological Modelling Instrument[J]. *Irrigation and drainage*, *60*, 35–41.

Rakovec, O., Weerts, A., Sumihar, J., & Uijlenhoet, R. (2015). Operational aspects of asynchronous filtering for flood forecasting. *Hydrology and Earth System Sciences*, *19*(6), 2911–2924. https://doi.org/10.5194/hess-19-2911-2015

Refsgaard, J. C., van der Sluijs, J. P., Brown, J., & van der Keur, P. (2006). A framework for dealing with uncertainty due to model structure error. *Advances in Water Resources*, *29*(11), 1586–1597. https://doi.org/10.1016/j.advwatres.2005.11.013

Reichle, R. H., McLaughlin, D. B., & Entekhabi, D. (2002). Hydrologic data assimilation with the ensemble Kalman filter. *Monthly Weather Review*, *130*(1), 103–114. https://doi.org/10.1175/1520-0493(2002)130%3C0103:HDAWTE%3E2.0.CO;2

Reichle, R. H., Walker, J. P., Koster, R. D., & Houser, P. R. (2002). Extended versus ensemble Kalman filtering for land data assimilation. *Journal of Hydrometeorology*, *3*(6), 728–740. https://doi.org/10.1175/1525-7541(2002)003%3C0728:EVEKFF%3E2.0.CO;2

Renard, B., Kavetski, D., Kuczera, G., Thyer, M., & Franks, S. W. (2010). Understanding predictive uncertainty in hydrologic modeling: The challenge of identifying input and structural errors. *Water Resources Research*, *46*, W05521. https://doi.org/10.1029/2009WR008328

Roth, M., Fritsche, C., Hendeby, G., & Gustafison, F. (2015, 31 Aug.–4 Sept. 2015). The ensemble Kalman filter and its relations to other nonlinear filters. Paper presented at the 2015 23rd European Signal Processing Conference (EUSIPCO), Nice, France.

Shen, Z., Chen, L., & Chen, T. (2012). Analysis of parameter uncertainty in hydrological and sediment modeling using GLUE method: A case study of SWAT model applied to Three Gorges Reservoir Region, China. *Hydrology and Earth System Sciences*, *16*(1), 121–132. https://doi.org/10.5194/hess-16-121-2012

Shi, P., Zhou, M., Qu, S., Chen, X., Qiao, X., Zhang, Z., & Ma, X. (2013). Testing a conceptual lumped model in karst area, southwest China. *Journal of Applied Mathematics*, *2013*, 10.

Smith, P., Beven, K., Weerts, A., & Leedal, D. (2012). Adaptive correction of deterministic models to produce probabilistic forecasts. *Hydrology and Earth System Sciences*, *16*(8), 2783–2799. https://doi.org/10.5194/hess-16-2783-2012

Sophocleous, M. (2002). Interactions between groundwater and surface water: The state of the science. *Hydrogeology Journal*, *10*(1), 52–67. https://doi.org/10.1007/s10040-001-0170-8

St-Pierre, M., & Gingras, D. (2004). Comparison between the unscented Kalman filter and the extended Kalman filter for the position estimation module of an integrated navigation information system. Paper presented at the Intelligent Vehicles Symposium, Parma, Italy.

Stricker, J., & Warmerdam, P. (1982). Estimation of the waterbalance in the Hupselse Beek basin over a period of three years and a first effort to simulate the rainfall-runoff process for a complete year. Paper presented at the Hydrological Research Basins and their Use in Water Resources Planning: Proceedings of the International Symposium, Berne, Switzerland.

Sugawara, M. (1974). Tank model and its application to Bird Creek, Wollombi Brook, Bikin River, Kitsu River, Sanaga River and Nam Mune. *Research Notes of the National Research Center for Disaster Prevention*, *11*, 1–64.

Sun, Y., Bao, W., Jiang, P., Ji, X., Gao, S., Xu, Y., et al. (2018). Development of multivariable dynamic system response curve method for real-time flood forecasting correction. *Water Resources Research*, *54*, 4730–4749. https://doi.org/10.1029/2018WR022555

Sun, Y., Bao, W., Jiang, P., Si, W., Zhou, J., & Zhang, Q. (2018). Development of a regularized dynamic system response curve for real-time flood forecasting correction. *Water*, *10*(4), 450. https://doi.org/10.3390/w10040450

Thompson, J. R., Sørenson, H. R., Gavin, H., & Refsgaard, A. (2004). Application of the coupled MIKE SHE/MIKE 11 modelling system to a lowland wet grassland in southeast England. *Journal of Hydrology*, *293*(1-4), 151–179. https://doi.org/10.1016/j.jhydrol.2004.01.017

Uhlenbrook, S., Seibert, J., Leibundgut, C., & Rodhe, A. (1999). Prediction uncertainty of conceptual rainfall-runoff models caused by problems in identifying model parameters and structure. *Hydrological Sciences Journal*, *44*(5), 779–797. https://doi.org/10.1080/02626669909492273

van Leeuwen, P. J. (1999). Comment on "Data assimilation using an ensemble Kalman filter technique". *Monthly Weather Review*, *127*(6), 1374–1377. https://doi.org/10.1175/1520-0493(1999)127%3C1374:CODAUA%3E2.0.CO;2

Verkade, J. S., Brown, J. D., Reggiani, P., & Weerts, A. H. (2013). Post-processing ECMWF precipitation and temperature ensemble reforecasts for operational hydrologic forecasting at various spatial scales. *Journal of Hydrology*, *501*, 73–91. https://doi.org/10.1016/j.jhydrol.2013.07.039

Vrugt, J. A., Gupta, H. V., Bouten, W., & Sorooshian, S. (2003). A Shuffled Complex Evolution Metropolis algorithm for optimization and uncertainty assessment of hydrologic model parameters. *Water Resources Research*, *39*(8), 1201. https://doi.org/10.1029/2002WR001642

Vrugt, J. A., ter Braak, C. J., Clark, M. P., Hyman, J. M., & Robinson, B. A. (2008). Treatment of input uncertainty in hydrologic modeling: Doing hydrology backward with Markov chain Monte Carlo simulation. *Water Resources Research*, *44*, W00B09. https://doi.org/10.1029/2007WR006720

Wang, C.-H., & Bai, Y.-L. (2008). Algorithm for real time correction of stream flow concentration based on Kalman filter. *Journal of Hydrologic Engineering*, *13*(5), 290–296. https://doi.org/10.1061/(ASCE)1084-0699(2008)13:5(290)

Weerts, A. H., & el Serafy, G. Y. (2006). Particle filtering and ensemble Kalman filtering for state updating with hydrological conceptual rainfall-runoff models. *Water Resources Research*, *42*, W09403. https://doi.org/10.1029/2005WR004093

Weerts, A. H., Winsemius, H. C., & Verkade, J. S. (2011). Estimation of predictive hydrological uncertainty using quantile regression: Examples from the National Flood Forecasting System (England and Wales). *Hydrology and Earth System Sciences*, *15*(1), 255–265. https://doi.org/10.5194/hess-15-255-2011

Welch, G., & Bishop, G. (1995). An introduction to the Kalman filter: University of North Carolina at Chapel Hill.

Werner, M., Schellekens, J., Gijsbers, P., van Dijk, M., van den Akker, O., & Heynert, K. (2013). The Delft-FEWS flow forecasting system. *Environmental Modelling & Software*, *40*, 65–77. https://doi.org/10.1016/j.envsoft.2012.07.010

Wilby, R. L. (2005). Uncertainty in water resource model parameters used for climate change impact assessment. *Hydrological Processes: An International Journal*, *19*(16), 3201–3219. https://doi.org/10.1002/hyp.5819

Wilks, D. S. (2011). *Statistical methods in the atmospheric sciences* (Vol. 100). New York: Academic press.

Winter, T. C., Rosenberry, D. O., & Sturrock, A. M. (1995). Evaluation of 11 equations for determining evaporation for a small lake in the north Central United States. *Water Resources Research*, *31*(4), 983–993. https://doi.org/10.1029/94WR02537

Wu, M., & Smyth, A. W. (2007). Application of the unscented Kalman filter for real-time nonlinear structural system identification. *Structural Control and Health Monitoring*, *14*(7), 971–990. https://doi.org/10.1002/stc.186

Xie, X., & Zhang, D. (2010). Data assimilation for distributed hydrological catchment modeling via ensemble Kalman filter. *Advances in Water Resources*, *33*(6), 678–690. https://doi.org/10.1016/j.advwatres.2010.03.012

Xu, C. Y., & Singh, V. P. (2000). Evaluation and generalization of radiation-based methods for calculating evaporation. *Hydrological Processes*, *14*(2), 339–349. https://doi.org/10.1002/(SICI)1099-1085(20000215)14:2%3C339::AID-HYP928%3E3.0.CO;2-O

Yang, J., Reichert, P., Abbaspour, K. C., & Yang, H. (2007). Hydrological modelling of the Chaohe Basin in China: Statistical model formulation and Bayesian inference. *Journal of Hydrology*, *340*(3–4), 167–182. https://doi.org/10.1016/j.jhydrol.2007.04.006

Zhang, Q., Gemmer, M., & Chen, J. (2008). Climate changes and flood/drought risk in the Yangtze Delta, China, during the past millennium. *Quaternary International*, *176*, 62–69.

Zhao, R. J. (1992). The Xinanjiang model applied in China. *Journal of Hydrology*, *135*(1), 371–381.